Structural Description of the $Na_2B_4O_7-Na_3AlF_6-TiO_2$ System. 1. IR and Raman Study of the Solidified Melts

Elena M. Anghel,[†] Pierre Florian,[‡] and Catherine Bessada*[,‡]

Institute of Physical Chemistry "Ilie Murgulescu" of Romanian Academy, Spl. Independentei 202, 060021 Bucharest, Romania, and Centre de Recherche sur les Matériaux à Haute Température, CRMHT-CNRS, 1D, Avenue de la Recherche Scientifique, 45071 Orléans, Cedex 2, France

Received: March 30, 2006; In Final Form: August 21, 2006

The pseudo-binary $Na_2B_4O_7-[Na_3AlF_6-TiO_2]_{11}$ system has been investigated at room temperature by means of X-ray diffraction, IR, Raman, and UV−vis spectroscopies. Evolution of the different spectra with $Na_2B_4O_7$ and TiO_2 contents evidenced the breaking-up of the large borate rings in favor of small borate units, the diminution of the B_{IV} fraction, and the partial substitution of oxygen by fluorine with the formation of oxyfluoride species. Two domains of compositions are described: a TiO_2-rich region with 20−50% $Na_2B_4O_7$ with the lowering of boron coordination and formation of $Ti(O,F)_6$ units and a TiO_2-poor region with 60−90% $Na_2B_4O_7$ where the Na_3AlF_6 modifier behavior is predominant. The enhanced modifier effect of $[Na_3AlF_6-TiO_2]_{11}$ in comparison with pure Na_3AlF_6 on the vitreous network of $Na_2B_4O_7$ consists of fluorine preference for binding to higher strength cations, Ti^{4+}, over Al^{3+} and Na^+ respectively, when TiO_2 addition exceeds 5 wt %.

1. Introduction

Melts belonging to the quaternary $NaCl-Na_3AlF_6-Na_2B_4O_7-TiO_2$ system are of particular interest because of their potentiality in the industrial production of high purity TiB_2 powders.[1,2] The underlying electrosynthesis mechanism is believed to involve discharge of BF_4^- and TiF_6^{2-} anions at the cathode.[2] Nevertheless, no studies have been performed yet to elucidate the nature of the species present in these melts. Moreover, the glass forming abilities of the electroactive $Na_2B_4O_7$ and TiO_2 components[3−6] would suggest diversity in terms of the coordination number of the species involved. Previous spectroscopic and thermodynamical studies of cryolitic melts[7−10] have already shown that three types of aluminum environments are to be expected: AlF_4^-, AlF_5^{2-}, and AlF_6^{3-}. A quantification of those species as well as a description of oxyfluoro-environments resulting from addition of Al_2O_3 in the melt have also been given by in situ high-temperature NMR.[9] Those results suggest therefore a more complex behavior in terms of the species present in the quaternary melts than the one developed up to now.

Our previous studies[11−14] have been focused on the subsystems $Na_2B_4O_7-Na_3AlF_6$ and $Na_2B_4O_7-[Na_3AlF_6-TiO_2]_e$ (where e stands for "3.5% TiO_2", i.e., the eutectic Na_3AlF_6/TiO_2 = 96.5:3.5 composition[15]) in an attempt to evidence the interactions between the $NaCl-Na_3AlF_6$ solvent and electroactive $Na_2B_4O_7-TiO_2$ components. No significant structural differences could be seen between these two subsystems, and for both, the only glass modifier component was Na_3AlF_6 and small TiO_2 additions seemed to preserve the vitreous structure of $Na_2B_4O_7$. The devitrification mechanism of the $Na_2B_4O_7-Na_3AlF_6$ mixtures has been shown by NMR[14] to proceed with a lowering of the boron coordination number and formation of the oxyfluoride species BOF_2.

The present study extends the prior ones by exploring the pseudo-binary $Na_2B_4O_7-[Na_3AlF_6-TiO_2]_{11}$ (where 11 is the wt % of TiO_2 in $Na_3AlF_6-TiO_2$) away from the aforementioned eutectic composition. The rather limited solubility domain of TiO_2 in Na_3AlF_6[15] should nevertheless be kept in mind because it has been reported[1] that very pure TiB_2 powders could be obtained only with compositions within the atomic ratio B/Ti = 12 to 20. We use here room-temperature vibrational spectroscopy (IR and Raman), UV−vis spectroscopy, and X-ray diffraction (XRD) on quenched samples to characterize the nature of the species present in solids and possible in the high-temperature melts. These spectroscopic methods have been already extensively used to characterize borate systems,[16−22] and this will lay the basis of our study dedicated to complex compounds. To investigate the glassy nature of the quenched samples and the crystalline phases grown during sample premelting, mixtures were analyzed by XRD. NMR has also been very successful in instigating borates,[23,24] and it will be the subject of a forthcoming part 2 of this paper.

2. Experimental Section

$NaBF_4$ and Na_2TiF_6 (Acros, 98% of purity and all reagent grade), Na_3AlF_6 (Merck), TiO_2 (Merck), and $Na_2B_4O_7 \cdot 10H_2O$ (Reactivul Bucharest) were used as starting materials. Anhydrous $Na_2B_4O_7$ was prepared from Borax as reported elsewhere.[14] The various mixtures (see Table 1 for compositions) were homogenized, melted, quenched, ground, and stored in a drybox. All compositions will be represented by wt % throughout this paper unless specified otherwise.

The IR spectra were recorded by means of a Carl Zeiss Jena type M80 spectrometer within a 4000−200 cm^{-1} range and on CsI pellets. These pellets were obtained for each sample by mixing 1 mg of the appropriate powder with 200 mg CsI.

* Corresponding author. E-mail: bessada@cnrs-orleans.fr. Fax: +33-(0) 238 638 103.

[†] Institute of Physical Chemistry "Ilie Murgulescu" of Romanian Academy.

[‡] Centre de Recherche sur les Matériaux à Haute Température.

10.1021/jp061977e CCC: $37.00
Published on Web 01/11/2007

TABLE 1: Nominal Compositions and Atomic Ratio B/Ti for the Ternary Samples: $Na_2B_4O_7$:[$Na_3AlF_6-TiO_2$]$_x$ (where *x* Stands for 11 wt % TiO_2)

sample	$Na_2B_4O_7$:Na_3AlF_6:TiO_2 wt %	$Na_2B_4O_7$:Na_3AlF_6:TiO_2 mol %	B/Ti
0T11	0:89:11	0:75.49:24.51	0
20T11	20:71.2:8.8	18.11:61.82:20.07	3.60
40T11	40:55.4:6.6	37.22:47.38:15.40	9.66
50T11	50:44.5:5.5	46.94:40.04:13.02	14.42
60T11	60:35.2:4.4	57.03:32.43:10.54	21.64
80T11	80:17.8:2.2	77.96:16.62:5.42	57.53
100T11	100:0:0	100:0:0	

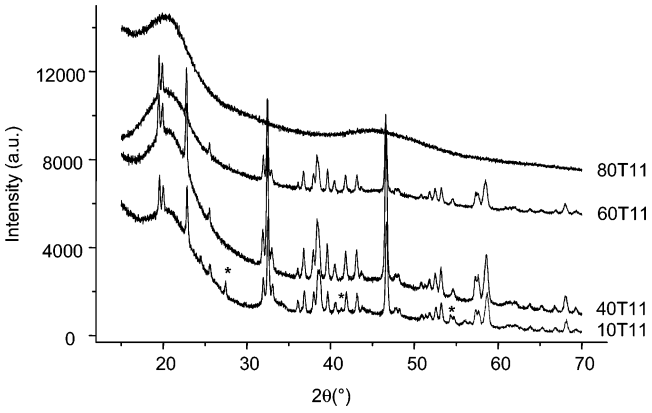

Figure 1. XRD patterns of selected compositions in the $Na_2B_4O_7-[Na_3AlF_6-TiO_2]_{11\%}$ system. The marked peaks correspond to the diffraction from the rutile TiO_2 crystal.

The Raman experiments were done by using the Renishaw System 2000 equipped with a Leica DMLM microscope (50×). Samples were excited with an argon ion laser operating at 488 nm with a typical output of 6.0 mW. Raman scattered spectra were collected along the same optical path as the incoming laser, at room temperature, with a charge-coupled device (CCD) detector array. The spectral data were analyzed with Renishaw v.1.2 WIRE software coupled with the GRAMS/32 C suite program. None of the spectra were smoothed. The spectrometer resolution was 1 cm^{-1} for the 15 μm slit-width used in measurements. The solid disks were obtained by pouring melts into a preheated copper mold with 1 cm diameter.

The UV−vis absorption spectra were collected within the 200−2000 nm range with a JASCO spectrometer type V-570 equipped with a large integrating sphere for solid samples. Mixtures used in UV−vis measurements were premelted in the same way as for IR pellets.

Powder diffraction data were collected with a D8 Advance Bruker AXS X-ray diffractometer, equipped with the linear detector Vantec-1, in the Bragg−Brentano configuration. The diffraction patterns were taken between 15 and 70° (2θ) with a step of 0.0164° and a count time of 1 s per step, using Cu Kα 1.2 radiation. An airtight specimen holder with an X-ray transparent cap was used. The sample was rotated at 15 rpm during data collection.

3. Results and Discussion

3.1. XRD. The X-ray diffraction patterns (Figure 1) show the presence of crystalline Na_3AlF_6 superimposed with an amorphous contribution. At high content of TiO_2, in the 10T11 sample premelted above its melting point (952 °C), the contribution of rutile TiO_2[25,26] is also detected (asterisk in Figure 1). At low TiO_2 content, this contribution is no more detectable in agreement with the insertion of Ti^{4+} in the glassy network. The 80T11 curve corresponds to a typical glassy structure. The presence of Anatase is difficult to state unambiguously, because its major peak ((101) at 25.325°) would coincide with one peak of the cryolite. Given the fact that F^- ions were found[27] to suppress the formation of brookite in TiO_2 powders doped with fluorides, it is not surprising that no brookite was noticed on the X-ray pattern of all ternary mixtures.

3.2. IR Spectra. IR spectra of $Na_2B_4O_7-[Na_3AlF_6-TiO_2]_{11}$ mixtures are presented in Figure 2 for compositions ranging 0−100% of $Na_2B_4O_7$. It is well-known that difficulties in interpreting such spectra arise from the vitreous nature of the samples, the multitude of possible structural groups (Figure 3), or even spectral distortions[21] due to intermediate TO−LO modes.[17] Nevertheless, three distinct regions can be related to vibration modes belonging to different borate species:[16,17] (i) 1500−1200 cm^{-1}, (ii) 1200−800 cm^{-1}, and (iii) 800−600 cm^{-1}. Literature data[16−19] can help to assess middle range order, i.e., rings built of 3-fold coordinated (B^{III}) and 4-fold coordinated (B^{IV}) boron (Table 2). Concurrently vibrational spectra of the 4- and 6-fold coordinated Al and Ti complexes lie below 800 cm^{-1}.

(i) In the 1500−1200 cm^{-1} region, the stretching modes of $B-O^b$ and $B-O^{nb}$ appear in 3-fold $B-\{O^b\}_3$ and $B-\{O^b\}_2-\{O^{nb}\}^-$ units (where b and nb stand for bridging and nonbridging, respectively). Hence, the broad band peaking down at 1340 cm^{-1} in Figure 2 could originate from the asymmetric stretching of borate rings.[16,19] Formation of oxyfluoro units of the 3-fold boron atoms was previously revealed[14] by NMR spectroscopy in the binary $Na_2B_4O_7-Na_3AlF_6$. However, gradual substitution of oxygen by fluorine around trigonal boron atoms should cause a shift of the 1340 cm^{-1} band toward higher wavenumbers,[28] which is hard to state from the IR spectra of these mixtures. Contributions from asymmetric B^{III} units not belonging to rings (Table 2) are also included in this band.

(ii) The 1200−800 cm^{-1} region generally corresponds to the $B-O^b$ stretching modes of B^{IV} units. Because fluorine is present in the compositions under discussion here, several species can be involved in this frequency range: diborate rings[19] and BO_3F groups.[28,29] A slight intensity decrease of this frequency region with respect to the aforementioned one can be noticed with increasing the content of 0T11 $[Na_3AlF_6-TiO_2]_{11}$ and is directly related to a decrease of the N_4 amount of B^{IV} species. The small shoulder observed at 1070 cm^{-1} can be attributed to BF_4^- anions[28−30] and isolated $(OAlF)_2$ complexes;[20] the one around 935 cm^{-1} can be attributed to B−O stretching of B_{IV} units in diborate groups (Table 2). The oxyfluoroborate species involved here weaken the glass network structure and are formed according to the following reactions:

$$\begin{cases} BO_4 + xF^- \rightarrow BO_{(4-y)}F_y + yO^{nb} & (1) \\ B(O,F)_4 \rightarrow B(O,F)_3 + (O,F)^{nb} & (2) \end{cases} \qquad \text{with } y = 1,...,4$$

(iii) In the 800−600 cm^{-1} region, one finds the bending vibrational mode between the two sp^2 borons $B-O^b-B$ at 720 cm^{-1} but also the B−F bond absorption at 780 cm^{-1} especially in the $[Na_3AlF_6-TiO_2]_{11}$-rich mixtures. The asymmetric vibration of AlO_4 units[20] as well as those related to TiO_4 units[31] can also be noticed within the 750−850 cm^{-1} range, making the assignment of the observed asymmetric band peaking down at 720 cm^{-1} rather ambiguous. Because AlO_4 units have been evidenced in the binary $Na_2B_4O_7-Na_3AlF_6$ system,[14] it is expected to have them present in the samples under investigation. Beyond the three regions characteristic of the borate structure, below 700 cm^{-1}, all the IR spectra exhibit the cryolite[32] signature (Figure 2).

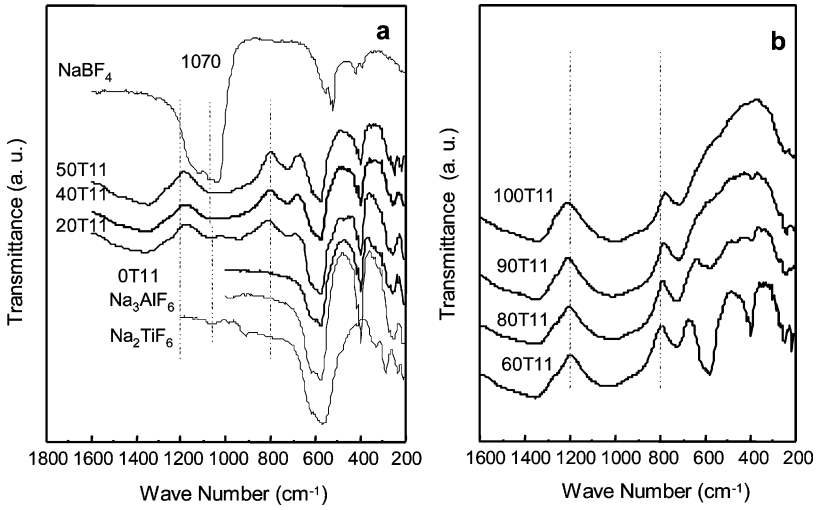

Figure 2. IR spectra recorded in the $Na_2B_4O_7-[Na_3AlF_6-TiO_2]_{11\%}$ system: (a) 0 to 50 wt % $Na_2B_4O_7$; (b) 60−100 wt % $Na_2B_4O_7$.

TABLE 2: Assignments of the IR Bands for the $Na_2B_4O_7-[Na_3AlF_6\text{-}TiO_2]_{11}$ System

peak position (cm^{-1})	assignment	ref
1500−1200	BO_3 stretching	16
1420−1500	B−O^- bonds	16
1390	BO_2F groups	25
1340	B−O asymmetric stretching of the different borate rings	16, 19
1260	tri-, tetra-, and pentaborate groups	16
1200−800	BO_4 stretching	16
900−1000	diborate rings	16
1000	$(^-O)_3BF$	25
1070	Al−O stretching vibration in $(OAlF)_2$, B−F stretching vibration in $[BF_4]^-$	20, 30
940	loose diborate rings	16
800−600	B−O−B bending	16
800	Al−O asymmetric vibration of $[AlO_4]^{5-}$	20
770	Ti−O stretching vibration in $[TiO_4]^{4-}$	31
615, 600	Ti−F stretching in $[TiF_6]^{2-}$	38
568	Al−F stretching frequency of $[AlF_6]^{3-}$	32
533	F−B−F bridges in $[BF_4]^-$	30
387	F−Al−F bending vibration of $[AlF_6]^{3-}$	32
371	O−Ti−O bending of $[TiO_4]^{4-}$	31
315, 281	F−Ti−F bending in $[TiF_6]^{2-}$	38

Compared with the IR spectra of $Na_2B_4O_7-[Na_3AlF_6-TiO_2]_e$ in the 0−50% $Na_2B_4O_7$ range, the mostly altered band (in shape and intensity) upon increasing the TiO_2 content is the one related to B^{IV}. This is to be related to Clayden's finding[33] in barium borates where the presence of low TiO_2 content (i.e., presence of TiO_4 units) promotes the formation of B^{IV}-bearing groups whereas at high content (i.e., presence of TiO_6^{2-} units) more B^{III}-bearing species can be found. If N_4 is therefore also found here to be sensitive to the balance between 4- and 6-fold coordinated titanium, it should be noticed that the coordination state of aluminum and fluorine present in our mixtures may play an important role as well. Focusing on the amount of TiO_2 in the mixture, we can divide the compositional range into (a) a TiO_2-rich region with 20−50% of $Na_2B_4O_7$ where Ti^{VI} units can be formed according to

$$TiO_{4/2} + 2B(O,F)_4 \rightarrow Ti(O,F)_6 + 2BO_3 \qquad (3)$$

and (b) a TiO_2-poor region with 60−90% of $Na_2B_4O_7$ where the Na_3AlF_6 modifier behavior is predominant. Equation 3 takes into account the fact that there is a fluorine preference for higher field-strength cations,[34] which in our case is titanium.

3.3. Raman Spectra. Raman spectra of $Na_2B_4O_7-[Na_3AlF_6-TiO_2]_{11}$ mixtures are presented in Figure 4 for compositions ranging 40−100% of $Na_2B_4O_7$, and Table 3 summarizes the simulations obtained for three compositions chosen inside (50T11) and outside (40T11, 60T11) the optimum B/Ti ratio of 12 to 20. By analogy to IR spectra of borate glasses, Raman spectra can be divided into low-, middle-, and high-frequency regions.[21,22] Low-frequency spectra, including the boson peak region, were not recorded for the ternary mixtures under discussion. In addition, the first three spectral features of Raman spectra (see Figure 4) for compositions below 60% of $Na_2B_4O_7$, at 348, 390, and 552 cm^{-1}, represent the ν_5, ν_2, and ν_1 vibrations for the AlF_6^{3-} ions of A_{1g}, E_g, and F_{2g} symmetry, respectively,[7] and evidence the presence of crystalline Na_3AlF_6. For compositions above that threshold, a broad peak was present in the lower-frequency envelope at about 500 cm^{-1} that could tentatively be attributed to "isolated" penta-, tetra-, and diborate groups (see Figure 3).

The middle-frequency region, 700−950 cm^{-1}, is related to the super-structure (tri-, penta-, tetra-, diborate rings) associated with the presence of intermediate range order[21,22] in borate glasses. Most of the peak assignments evidenced by the simulation shown in Figure 3 and Table 3 are included in this region.

The weak feature at 717 cm^{-1} in 40T11 can be assigned to B_2OF_6 and $B_3O_3F_6$ (nonplanar rings);[28,29] similarly, the strong band at 766 cm^{-1} can be related not only to the rings with two BO_4 units, B_3O_8, but also to the $B_3O_3F_6$ rings made of three $(-O)_2BF_2$ groups. By analogy with the asymmetric band at 940 cm^{-1} in sodium borate glasses,[16] the peak at 930 cm^{-1} could arise from vibrations either of loose diborate rings or of orthoborate units, BO_3^{3-}, formed by breaking up $BO_{3,ring}$ units (i.e., B_3O_8 ring) as postulated by Sen[24] for alkali borate melts:

$$BO_{3,ring} \rightarrow BO_{3,non\text{-}ring} \qquad (4)$$

In our case, this reaction is controlled by the presence of glass modifiers. However, the absence of the strong Raman band at 895 cm^{-1} due to the symmetric stretching mode of B−O in orthoborate units[16] would invalidate their presence.

In this frequency region, a band around 890 cm^{-1} grows markedly upon increasing the $[Na_3AlF_6-TiO_2]_{11}$ content and can therefore be assigned to the Ti−O stretching mode of Ti^{IV}-bearing units.[4] This peak position is 10 cm^{-1} lower than the one observed previously[12] in $99Na_2B_4O_7.1TiO_2$, which would suggest a substitution of oxygen by fluorine around the

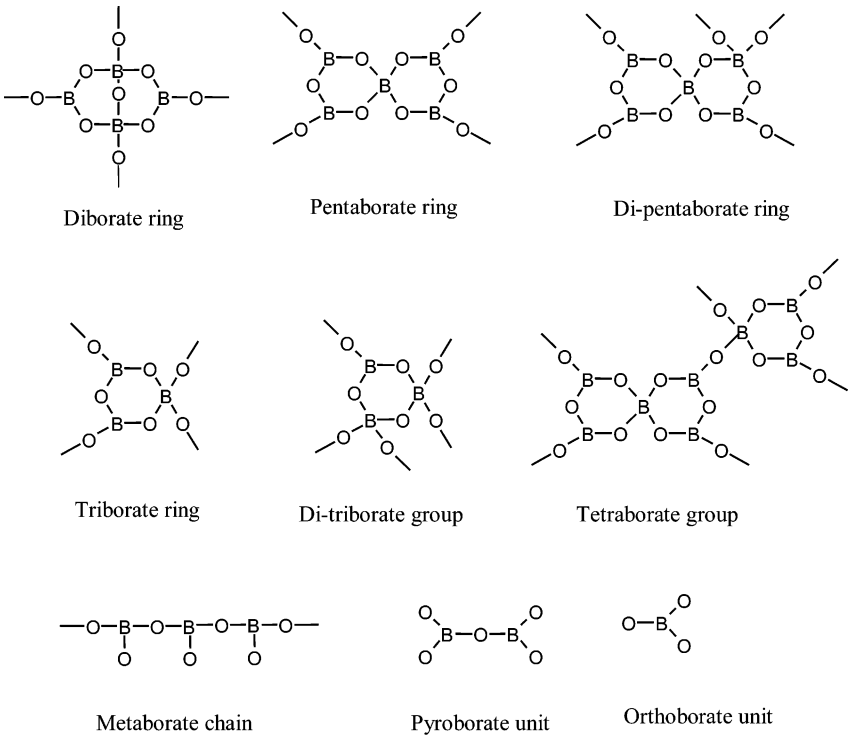

Figure 3. Schematic representations of the various borate groups discussed in this paper.

TABLE 3: Raman Peak Position and Assignment for the 40T11, 50T11, and 60T11 Mixtures

40T11	50T11	60T11	assignment	ref
348	348	348	AlF_6^{3-}	7
390	390	392	AlF_6^{3-}	7
552	552	555	AlF_6^{3-}	7
717			$B_2OF_6^{2-}$	25
	738	734	Ti−O stretching vibration in isolated TiO_4 tetrahedra	4
763	768	768	breathing vibration of the six-membered rings with one or two BO_4 (i.e., tri-, tetra-, or pentaborate groups)	16
884	890	890	Ti−O stretching modes of TiO_4	4
930	930	931	loose diborate rings or orthoborate units	16
	1077		B−F stretching vibration of BF_4 units	27
1238	1246	1297	$B-O^-$ stretching vibration in pyroborate units	16
1338	1339	1353	stretching of $B-O^-$ bonds attached to large borate segments (rings, metaborate chain)	16
1445	1440	1465	stretching of $B-O^-$ bonds attached to large borate segments (rings and chain type metaborate units)	16

tetrahedral titanium. Although a correlation between coordination number of titanium and Raman peak position is difficult to state, the Ti−O stretching mode over the 600−650 cm^{-1} range[4] can originate from TiO_6. Under this assumption, no direct evidence of TiO_6 units was visible in the Raman spectra of the two ternary glasses: 80T11 and 90T11; the presence of the six-coordinated titanium units can be masked by the very intense bands in the 580−1180 cm^{-1} region for the rest of the mixtures. Finally, the very weak contribution at 1070 cm^{-1} in the 50T11 spectrum (see the simulated spectrum in Figure 3) could point out the formation of BF_4^- ions.[30]

The next region from 1100 to 1600 cm^{-1} is associated in borate glasses with vibrational modes of short-range order.[21] Because the diborate rings[16] give a contribution at 1120 cm^{-1}, this region should be limited to 1150−1600 cm^{-1} in our case. If the diborate rings are then seen to be mostly present in the glassy samples 100T11 ($Na_2B_4O_7$), 90T11, and 80T11, the pyroborate units, B_2O_5,$^{4-}$ in contrast, are absent from these compositions and might appear in the nonglass forming compositions. However, formation of pyro-borates units in the high modifier $[Na_3AlF_6-TiO_2]_{11}$ content ternary compositions is invalidated by the absence of the strong Raman doublet at 820 and 1210 cm^{-1} typical of these units.[16] The band at 1370 cm^{-1} related[11] to single $Na_2B_4O_7$[14] and shifted toward lower frequency upon adding $[Na_3AlF_6-TiO_2]_{11}$ suggests a weakening of the borate structure by substitution of oxygen by fluorine. In the same frequency region, the band located between 1430 and 1490 cm^{-1} strongly increases with $[Na_3AlF_6-TiO_2]_{11}$ content and is related to the increase of the number of $B-O^-$ bonds attached to large borate rings or, in other words, to a decrease of the network connectivity. This behavior can be illustrated by the case of a di-triborate ring (showing up at 766 cm^{-1}) consisting of one $B-\{O^b\}_3$ and two $B-\{O^b\}_4$ units and undergoing the following reaction:

$$(B_3O_3O_5{}^b)^{2-} \rightarrow (B_3O_3O_3{}^bO^{nb})^{2-} + O^{nb} \qquad (5)$$

which converts a $B-\{O^b\}_4$ unit into a $\{O^b\}_2B-O^-$ species. The introduction of glass modifier cations (Na^+, Al^{3+}, Ti^{4+}) in the borate matrix yields therefore to the formation of small borate groups at the expense of large rings.

3.4. UV−Vis Spectra. The UV−vis spectra of $Na_2B_4O_7-[Na_3AlF_6-TiO_2]_{11}$ mixtures, displayed in Figure 5, clearly evidence the presence below 400 nm of the ligand-to-metal

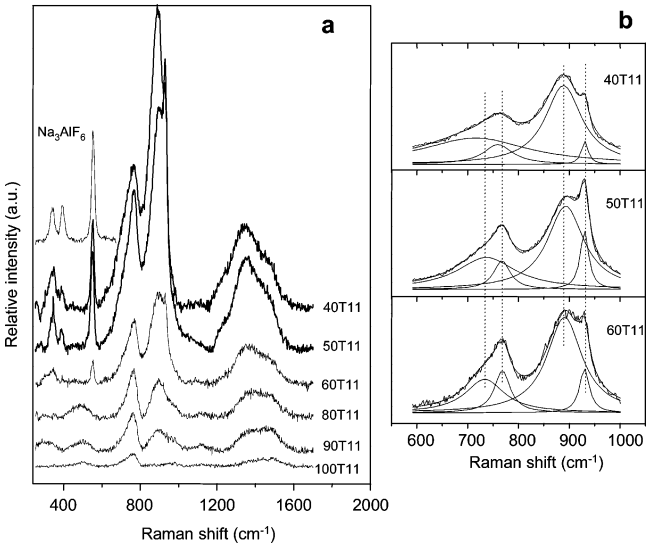

Figure 4. (a) Raman spectra of the $Na_2B_4O_7-[Na_3AlF_6-TiO_2]_{11\%}$ mixtures. (b) Simulations of the 50-, 40-, and 60T11 spectra.

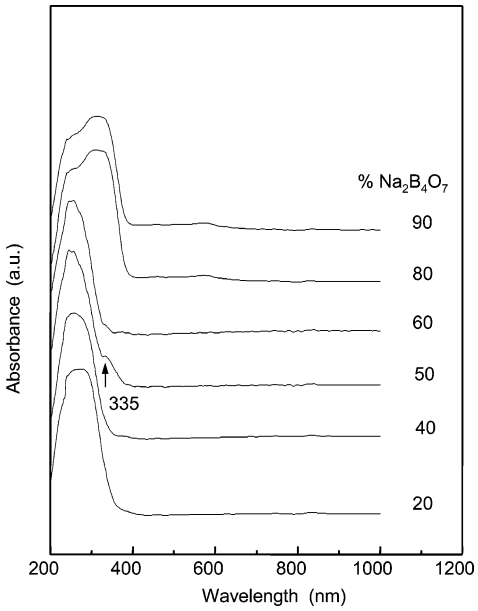

Figure 5. UV−vis spectra of $Na_2B_4O_7-[Na_3AlF_6-TiO_2]_{11\%}$ system.

charge-transfer band[35,36] of Ti^{4+} in either tetrahedral or octahedral symmetry. Band position within 250−270 nm is characteristic to the polymerized six-coordinated Ti^{4+} species.[36] Concurrently, the band at about 330 nm was registered for the $Na_2B_4O_7$-rich mixtures. This position coincides with that observed for pure TiO_2. Fluorine influence over titanium surroundings in the case of the 50T11 and 0T11 mixtures might be inferred from the higher wavelength bands above 335 nm. This finding is analogous to the one for the TiO_2 powders doped with fluoride[37] where stronger absorption and an upshifted band gap transition were recorded. In contrast, neither the crystal field band $^2T_{2g} \rightarrow {}^2E_g$ or $^2B_{2g} \rightarrow {}^2B_{1g}$ and $^2B_{2g} \rightarrow {}^2A_{1g}$ transitions of Ti^{3+} ions in distorted octahedral sites[36] (within 400−560 nm and 540−660 nm, respectively) can be found in these spectra. This therefore invalidates the presence of Ti^{3+}-bearing species in distorted octahedral sites, and hence only Ti^{4+} cations are present over the whole concentration range explored here.

4. Conclusions

The multi-spectroscopic investigation of the pseudo-binary system $Na_2B_4O_7-[Na_3AlF_6:TiO_2]_{11\%}$ evidenced two domains of compositions corresponding to glass and nonglass forming mixtures as a result of cation ordering at fluorine sites. In the nonglass forming mixtures (with less than 50 wt % $Na_2B_4O_7$), the borate network is modified mainly by formation of oxy-fluoro-species and lowering boron coordination with Na_3AlF_6 and TiO_2 additions. Several borate oxyfluoro-species have been directly or indirectly depicted: tetrahedral species $B(O,F)_4$ but also triangular $B(O,F)_3$ ones possibly in the form of the nonplanar boroxy ring $B_3O_3F_6$. For the glass forming mixtures, a behavior analogous to that of the binary mixture $Na_3AlF_6-Na_2B_4O_7$ is noticed and mainly controlled by the influence of glassy network modifier addition. In the binary, the addition of cryolite was responsible for weaker connectivity in the glass and the formation of $B(O,F)_3$ units. In the ternary, the introduction of an additional glass modifier (higher than 5%) such as Ti^{4+} in the borate matrix promotes the formation of small borate groups at the expense of larger rings and thus also decreases the network connectivity. The lack of quantitative description of this multi-spectroscopic approach as well as of the molten phase in the pseudo-binary $Na_2B_4O_7-[Na_3AlF_6-TiO_2]_{11}$ will be improved in the second part of this paper by high resolution and high-temperature NMR spectroscopy.

Acknowledgment. We are grateful to Dr. A. Voice for access to Renishaw System 2000 at the Department of Physics and Astronomy of University of Leeds and to E. Veron from CRMHT, Orleans, for XRD measurements. This work has been financially supported by the EEC ARI contract HPRI-CT-1999-00042 and CNRS- Romanian Academy cooperation.

References and Notes

(1) Gomes, J. N.; Ukida, K. U.S. Patent 3,775,271, 1972.
(2) Makyta, M.; Danek, V.; Haarberg, M.; Thonstad, J. *J. Appl. Electrochem.* **1996,** *26*, 319−324.
(3) Zachariasen, W. H., *J. Am. Ceram. Soc.* **1932**, *54*, 3841−3846.
(4) Sakka, S.; Miyaji, F.; Fukumi, K. *J. Non-Cryst. Solids* **1989**, *112*, 64−68.
(5) Terashima, K.; Uchino, T.; Hasimoto, T.; Yoko, T. *J. Ceram. Soc. Jp.* **1997**, *105*, 288−293.
(6) Pernice, P.; Esposito, S.; Aronne, A. *Phys. Chem. Glasses* **1998**, *39*, 222−227.
(7) Gilbert, B.; Martene, T. *Appl. Spectrosc.* **1990**, *44*, 299−304.
(8) Robert, E.; Lacassagne, V.; Bessada, C.; Massiot, D.; Gilbert, B.; Coutures, J.-P. *Inorg. Chem.* **1999**, *38*, 214−217.
(9) Lacassagne, V.; Bessada, C.; Florian, P.; Bouvet, S.; Ollivier, B.; Coutures, J.-P.; Massiot, D. *J. Phys. Chem. B* **2002**, *106*, 1862−1868.
(10) Robert, E.; Olsen, J. E.; Danek, V.; Tixhon, E.; Ostvold, T.; Gilbert, B. *J. Phys. Chem. B* **1997**, 101, 9447−9457.
(11) Anghel, E. M.; Zaharescu, M.; Zuca, S.; Pavlatou, E. *J. Mater. Sci.* **1999**, *34*, 3923−3929.
(12) Anghel, E. M.; Pavlatou, E.; Balasoiu, M.; Zuca, S. *High Temp. Material Processes (N. Y.)* **2000**, *4*, 431−440.
(13) Anghel, E. M.; Balasoiu, M.; Zuca, S.; Segal, E. *High Temp.−High Pressures.* **2001**, *33*, 411−417.
(14) Bessada, C.; Anghel, E. M. *Inorg. Chem.* **2003**, *42*, 3884−3890.
(15) Madhavan, T. P.; Matiasovsky, K.; Danek, V. *Chem. Zvesti* **1971**, *25*, 253−258.
(16) Kamitsos, E. I., Karakassides, M. A.; Chryssikos, G. D. *J. Phys. Chem.* **1987**, *91*, 1073−1079. Kamitsos, E. I., Karakassides, M. A. *Phys. Chem. Glasses* **1989**, *30*, 19−26.
(17) Machowski, P. M., Varsamis, C. P. E., Kamitsos, E. I., *J. Non-Cryst. Solids* **2004**, *345/346*, 213−218. Kamitsos, E. I., Yiannopoulos, Y. D., Varsamis, C. P., Jain, H. *J. Non-Cryst. Solids* **1997**, *222*, 59−68.
(18) Aronne, A.; Esposito, S.; Pernice, P. *Phys. Chem. Glasses* **1999**, *40*, 63−68.
(19) Efimov, A. M. *J. Non-Cryst. Solids* **1999**, *253*, 95−118.
(20) Mausbach, K.; Nowack, N.; Schlegelmilch, F. *Steel Res.* **1993**, *5*, 239−245.

(21) Yano, T.; Kunimine, N.; Shibata, S.; Yamane, M. *J. Non-Cryst. Solids* **2003**, *321*, 137−146.
(22) Yano, T.; Kunimine, N.; Shibata, S.; Yamane, M. *J. Non-Cryst. Solids* **2003**, *321*, 157−168.
(23) Bray, P. J. *Inorg. Chim. Acta* **1999**, *289*, 158−173.
(24) Sen, S. *J. Non-Cryst. Solids* **1999**, *253*, 84−94.
(25) Lacks, D. L.; Gordon, R. G. *Phys. Rev. B: Condens. Matter*. **1993**, *48*, 2889−2908.
(26) Burdett, J. K.; Hughbanks, T.; Miller, G. J.; Richardson, J. W., Jr.; Smith, J. V.; *J. Am. Chem. Soc.* **1987**, *109*, 3639−3646.
(27) Yu, J. C.; Yu, J.; Ho, W.; Jiang, Z.; Zhang, L. *Chem. Mater*. **2002**, *14*, 3808−3816.
(28) Maya, L. *J. Am. Ceram. Soc.* **1977**, *60*, 323−328.
(29) Von Barner, J. H.; Andersen, K. B.; Berg, R. W. *J. Mol. Liq.* **1999**, *83*, 141−151.
(30) Quist, A. S.; Bates, B.; Boyd, G. E. *J. Chem. Phys.* **1971**, *54*, 4896−4901.
(31) Gonzalez-Vilchez, F.; Griffith, W. P. *J. Chem. Soc., Dalton Trans.* **1972**, 1416−1421.
(32) Reisfeld, M. G. *Spectrochim. Acta* **1973**, *29A*, 1923−1926.
(33) Clayden, N. J.; Esposito, S.; Arone, A.; Pernice, P. *J. Non-Cryst. Solids* **1999**, *249*, 99−105. Furukawa, T.; White, W. B. *Phys. Chem. Glasses* **1979**, *20*, 69−80.
(34) Kiczenski, T. J.; Du, L.-S.; Stebbins, J. F. *J. Non-Cryst. Solids* **2004**, *337*, 142−149.
(35) France, P. W.; Carter, S. F.; Parker, J. M. *Phys. Chem. Glasses* **1986**, *27*, 32−41.
(36) Mendez-Vivar, J.; Mendoza-Serna, R.; Bosch P.; Lara, V. H. J. *Non-Cryst. Solids* **1999**, *248*, 147−158.
(37) Hashimoto, T.; Uchida, H.; Takagi, I.; Nasu, H.; Kamiya, K. *J. Non-Cryst. Solids* **1999**, *253*, 30−36.
(38) Forrest, I. W.; Lane, A. P. *Inorg. Chem.* **1976**, *15*, 265−269